The Space Congress® Proceedings

1999 (36th) Countdown to the Millennium

Apr 27th, 2:00 PM

Paper Session I-B - Characterizing Space-Grown Degenerate Narrow Gap Semiconductors by Scanning Tunneling Optical Spectroscopy

J. D. Patterson
Florida Institute of Technology - Melbourne

Joel Blatt
Florida Institute of Technology - Melbourne

J. G. Mantovani
Florida Institute of Technology - Melbourne

Ryne Raffaelle
Florida Institute of Technology - Melbourne

Characterizing Space-Grown Degenerate Narrow Gap Semiconductors by Scanning Tunneling Optical Spectroscopy

by

J. D. Patterson, Joel Blatt, Jay Burns, J. G. Mantovani, and Ryne Raffaelle
Florida Institute of Technology
Melbourne, FL 32901-6988

Abstract

We consider the II-VI narrow gap semiconducting alloys $Hg_{(1-x)}Cd_{(x)}Te$, $Hg_{(1-x)}Zn_{(x)}Te$, $Hg_{(1-x)}Zn_{(x)}Se$, for which empirical equations exist that give each alloy's forbidden energy band gap $E_g(x)$ as a function of its stoichiometry as characterized by the value x. These materials are important to NASA for two reasons. They are useful for making infrared detectors, and they are best grown in microgravity to optimize their uniformity. The equations can be inverted to yield the stoichiometry parameter x provided that the value of E_g can be determined experimentally, for example, by optical absorption measurements. We have investigated an alternative method, which should yield appreciably better spatial resolution, in which scanning tunneling optical spectroscopy (STOS) is used to measure the enhancement of the current that is due to photoexcitation of carriers at the tunneling junction in an STM.

We present a simplified working model for low temperature calculations of STOS. Our major conclusions are: (a) for the degenerate case, knowledge of $N_D - N_A$ (donor density minus the acceptor density) can be used to deduce the true band gap from the apparent band gap, (b) the low temperature tunneling current may have a sharper onset, depending on the diffusion length, at the band gap than does the optical absorption, and (c) our simplified formulation allows for quick, straightforward evaluation of many different cases and is in essential agreement with more detailed analysis.

I. Introduction

Mercury Cadmium Telluride[1] and related substances are well known to be important for use as infrared detectors and related uses in space. Consequently, methods for characterizing these materials, as grown in microgravity (as for instance on the Space Shuttle) to improve uniformity, are becoming very important.[2] A straightforward, simplified working model for the optical absorption and tunneling current in STOS (scanning tunneling optical spectroscopy)[3,4] is presented for certain narrow gap compound semiconductors MCT (Mercury Cadmium Telluride), MZT (Mercury Zinc Telluride), and MZS (Mercury Zinc Sulfide). We consider the degenerate n-type case and use simplified expressions for the Fermi energy, the concentration of absorbed carriers which drift to the surface, the barrier for tunneling from the sample surface to the tip and the tunneling current. For the essential overall features, our results are valid only at very low temperature and compare well to a more complete analysis which we have done.[5] Using simple expressions and reasonable values for all needed parameters characterizing the materials, our results can be quickly obtained. No experimental results are yet available for actual photo induced tunneling current measurements, but our calculated optical absorption coefficients are in the correct experimental range.[6]

A planned use of these results is in conjunction with experiments to determine the true energy gap and thus the stoichiometry x. Empirical expressions for E_g *vs.* x for MCT, MZT, and MZS are given in Table I. The technique of extracting x from the measured energy gap applies to both optical absorption and STOS, but as we will show below, STOS may be preferred since the tunneling current seems to rise more steeply as a function of frequency at E_g than does absorption. The steep rise of the tunneling current should aid in determining the energy gap more precisely, and the spatial resolution of the STM should improve the localization of E_g and hence x.

Table 1. Representative Energy Gap Equations (E_g in eV)

MCT	$E_g(x,T) = -0.302 + 1.93(x) - 0.81(x^2) + 0.832(x^3) + 5.35(1-2x)(10^{-4})T$	Ref. 14
MCT	$E_g = q + f/h$, where $f = 1\times10^{-4}[6.3(1-x) - 3.25x - 5.92x(1-x)]T^2$, $h = 11(1-x) + 78.7x + T$, and $q = -0.303(1-x) + 1.606x - 0.132\,x(1-x)$	Ref. 15
MCT	$E_g(x,T) = -0.302 + 1.93(x) - 0.81(x^2) + 0.832(x^3) + 5.35\times10^{-4}(1-2x)(-1823 + T^3)/(255.2 + T^2)$	Ref.16
MCT	$E_g(x,T) = -0.295 + 1.87x - 0.28x^2 + 1\times10^{-4}(6 - 14x + 3x^2)T + 0.35x^4$	Ref. 17
MCT	$E_g(x,T) = 1.838x - 0.3424 + 0.148x^4 + (6.29\times10^{-2} + 7.6810\times10^{-4}T)(1-2.14x)/(1+x)$	Ref. 18
MCT	$E_g(x,T) = 1.858x - 0.304 + 0.054x^2 + 6.3x10^{-4}T^2(1-2.00x)/(11+T)$	Ref. 9
MZT	$E_g(x,T) = -0.3 + 3.24\times10^{-2}x^{1/2} + 2.731x - 0.629x^2 + 0.533x^3 + 5.3\times10^{-4}T(1 - 0.76x^{1/2} - 1.29x)$	Ref. 19
MZS	$E_g(x,T) = -0.222 + 5.41\times10^{-4}T + (2.205 - 1.35\times10^{-3}T)x + 0.96x^2$	Ref. 20

II. Degenerate Fermi Energies

Here, we assume absolute zero for convenience and simplicity. The energy depends only on the magnitude of the wave vector k, so if n is the number of electrons per unit volume in the conduction band, we know $k_F = (3\pi^2 n)^{1/3}$. From the Kane model [7], in the conduction band with $\Delta >> E_g$, and $\Delta >> P$, where Δ is the spin orbit parameter and P is the momentum matrix element, we have for the conduction band energy at absolute zero:

$$E = E_g + \frac{\hbar^2 k^2}{2m} + \frac{E_g}{2}\left(\sqrt{1 + \frac{8P^2k^2}{3E_g^2}} - 1\right) \qquad (1)$$

Evaluating this at the Fermi energy with $k = k_F$, and neglecting $\frac{\hbar^2 k_F^2}{2m}$ as small compared to the terms retained, we find:

$$E_F = \frac{E_g}{2}\left[1+\left(\sqrt{1+\frac{8P^2}{3E_g^2}\left(3\pi^2 n\right)^{2/3}}\right)\right] \tag{2}$$

A plot of the Fermi energy, as a function of effective doping density, for MCT with $x = 0.2$ is shown in Fig. 1. From E_F, straight-forward differentiation and rearrangement gives,

$$\delta E_F = \frac{2}{3}\frac{E_F}{n}\left(\frac{E_F - E_g}{2E_F - E_g}\right)\delta n_{ph} \tag{3}$$

which will be needed to compute the tunneling current.

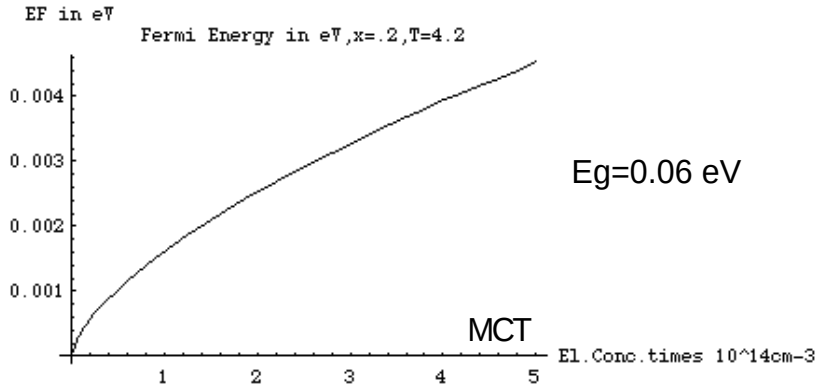

Fig. 1

The Fermi energy of MCT as a function of $N_D - N_A$ (at low temperature).

III. The Absorption Coefficient, α

Anderson[8] has given a relatively complete calculation of α for Mercury Cadmium Telluride, but the simplified analysis of Nathan[9] is useful for getting fairly accurate results quickly. Using Nathan's model, modified to include degeneracy as determined above, we have evaluated the absorption coefficient. Fig. 2, shows how, at very low temperatures, degenerate MCT has a cut-on frequency at a higher energy than the actual energy gap (Moss-Burstein effect).

In the calculation leading to Fig. 2, a net donor concentration typical for MCT was used.[10] If one can fit the experimental results for the degenerate case with proper $N_D - N_A$, then the energy gap and hence x can be determined with this simplified model.

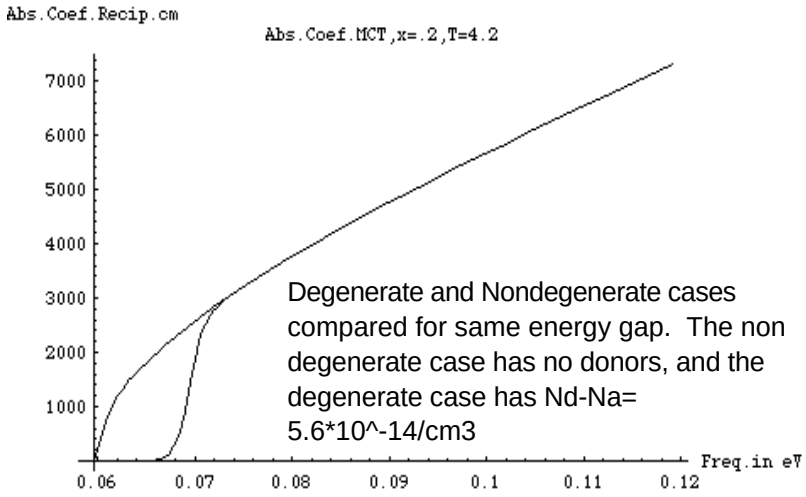

Fig. 2

Modified Nathan model for degenerate and non-degenerate optical absorption coefficients for MCT.

IV. The Carrier Concentration

We have shown [11] that an expression for the number of electrons that diffuse to the surface, due to photogenerated carriers within the bulk material, is given by:

$$\delta n_{ph} = \frac{\alpha I_o}{\hbar\omega S\left(\alpha + \frac{1}{L}\right)\left(1 + \frac{D}{LS}\right)} \tag{4}$$

where I_o is the intensity of incident light, D is the diffusion coefficient, S is the surface recombination velocity, τ is the recombination time, and the diffusion length is defined by $L^2 = D\tau$ (where minority or hole values, should presumably be used for all material parameters). For the case where $\alpha L << 1$ and $LS << D$, this expression simplifies to:

$$\delta n_{ph} = \frac{\alpha I_o \tau}{\hbar\omega} \tag{5}$$

Equation (4) was used in all the calculations.

V. Tunneling Barrier

For simplicity, we assume the barrier $V(z)$ is parabolic, with barrier height proportional to B,

$$V(z) = B\left(a^2 - z^2\right), \tag{6}$$

and as shown in Fig. 3. From the WKB approximation, the barrier transmission coefficient is,

$$T(W) = \exp\left[-2\left(\frac{2m}{h}\right)^{1/2}\int_{z_1}^{z_2}\sqrt{V(z)-W}\cdot dz\right] \qquad (7)$$

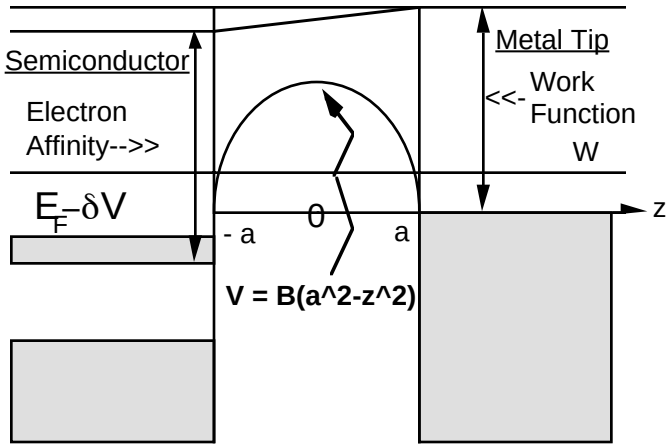

Fig. 3

Schematic of the tunneling barrier in STM.

For $V(z)$ as given by (6), this yields

$$T(W) = e^{-K_1+K_2W}, \qquad (8a)$$

where

$$K_1 = \sqrt{\frac{2m}{\hbar^2}}\pi a^2\sqrt{B}, \qquad (8b)$$

and

$$K_2 = \sqrt{\frac{2m}{\hbar^2 B}}\pi \quad . \qquad (8c)$$

In our calculations, the barrier height Ba^2 was chosen to be approximately equal to the work function of the tip (4.5 eV) and the sample-to-tip distance was $7\,\mathring{A}$.

VI. STOS Tunneling Current

From standard analysis using this tunneling probability (see *e.g.* Feenstra and Stroscio[12]), the tunneling current from the semiconductor conduction band is given by

$$J_{CB} = \frac{me}{2\pi^2\hbar^3}\int_{E_F-eV}^{E_F} dE\ \theta\left(E - E_{CB}\right) \int_{E\left(1-\alpha_{CB}\right)+\alpha_{CB}E_{CB}}^{E} T(W)\, dW\ ;\ E_{CB} = E_g,\ \alpha_{CB} = \frac{m_{CB}}{m}. \quad (9)$$

As usual, $\Theta(x) = 1,\ x > 0$, and $\Theta(x) = 0,\ x < 0$. For $E_F > E_g$, Eqn. (9) gives for J_{CB}, if we let $-eV \rightarrow \delta E_F <<< E_F$ (it is assumed that the excess photogenerated carriers in the semiconductor, which shift the quasi Fermi energy, act like an applied voltage, which similarly shifts the relative quasi Fermi energies):

$$J_{CB}^{photoexcited} = \frac{me}{2\pi^2\hbar^3}\frac{e^{-K_1}}{K_2}\left(e^{K_2E_F} - e^{K_2E_F\left(1-\alpha_{CB}\right)-\alpha_{CB}K_2E_g}\right)\delta E_F \quad (10)$$

where δE_F can be evaluated from δn due to photoexcitation (see Eq. 3). We consider only electron conduction, because in the n-type cases that we have treated, more extensive analysis[5] shows that the light and heavy hole currents are negligible. Typical values for material constants that we used are also contained in the more extensive analysis.[5] Briefly, representative values for MCT are: $\Delta = 1.0$ eV, $P = 8.5\times10^{-8}$ eVcm, $\frac{m_{hh}}{m_e} = 0.53$, $\varepsilon_\infty = 15.2 - 15.6x + 8.2x^2$ (Gaussian), $S = 10\frac{m}{s}$, $D = 0.3\frac{m}{s^2}$, and $\tau = 10^{-7}$s. Results of our calculation for two different degeneracies is shown in Figure 4. Figure 5 Shows the effect of changing diffusion length. The cut-on of the current is sharpest when $L\alpha$ increases.

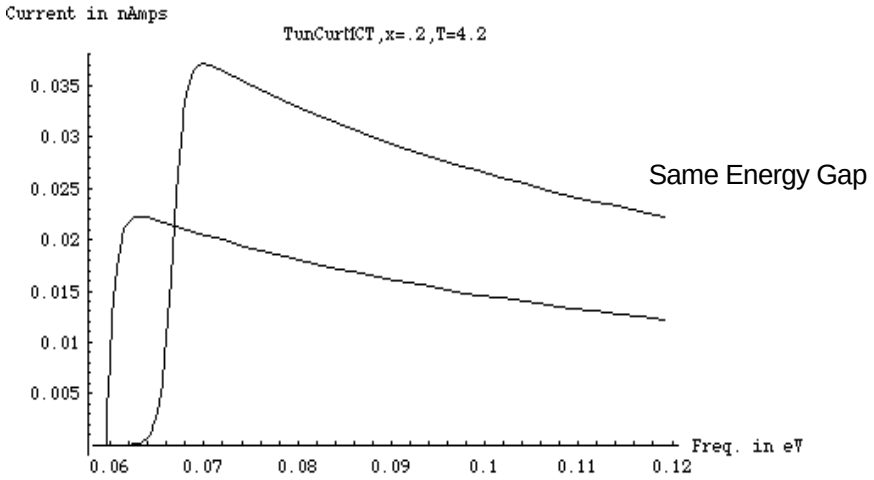

Fig. 4

Tunneling current in STOS for two degenerate cases for STM. STOS for MCT using absorption coefficient from simplified method of V. Nathan. The top curve has $N_D - N_A = 5.6\times10^{14}/\text{cm}^3$ and the bottom curve has $N_D - N_A = 5.6\times10^{13}/\text{cm}^3$. As usual, the current is somewhat arbitrary as it depends on the area of current flow and the intensity of light. These were the same for both curves, however. The more degenerate curve has more current because the tunneling barrier is less at higher degeneracy. We have assumed, at each frequency, 1 milliwatt of power from a laser. Then, we assume the ratio of current gathering area to the area of light illumination to be 10^{-6}.

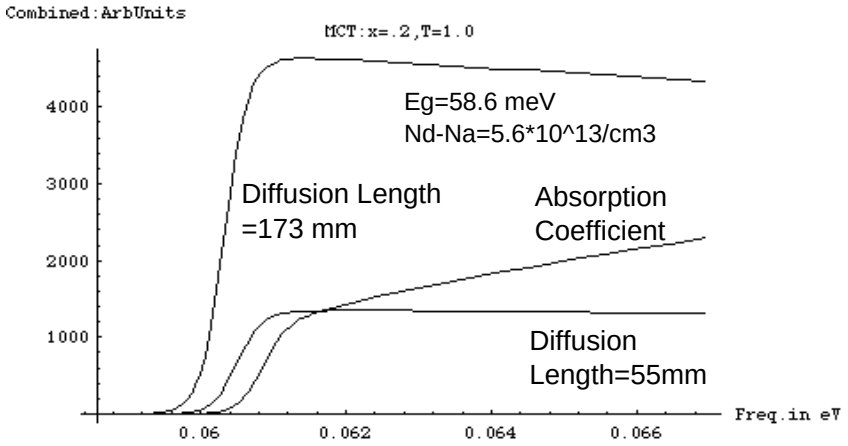

Fig. 5

Tunneling current in STOS for two different diffusion lengths. For comparison, the absorption coefficient is also shown.

VII. Discussion of Results

Our major conclusions are: (1) For the degenerate case, knowledge of $N_D - N_A$ (the donor density minus the acceptor density) is necessary to deduce the true band gap from the apparent band gap, and (2) for large diffusion lengths (actually $L\alpha >> 1$), the low temperature tunneling current has a distinctly sharper onset at the band gap than does the optical absorption. (3) In general one can show that when $L\alpha >> 1$ the tunneling current is almost independent of a non vanishing absorption coefficient, while for $L\alpha << 1$ the tunneling current is proportional to $\frac{\alpha}{\omega}$. (4) Finally, due to the localized nature of STM, we expect (although our analysis here does not address this point) that STOS will given much better spatial resolution in characterizing how x varies with position. In fact, this was our original motivation. Our simplified formulation allows for quick evaluation of many different cases and is in essential agreement with more detailed analysis.

It should also be pointed out that below the band gap, MCT has been found to have a modified Urbach tail[13] (which seems to be valid for $\alpha \leq 500$ cm^{-1}). These tailing effects in the absorption coefficient, can be due to a variety of causes, such as lattice disorders and impurities. For the simplified analysis presented here, we have neglected such effects.

Acknowledgements

This work has been supported by the Universities Space Research Association (USRA) through subcontract 3537-000-05 for cooperative agreement NCC8-66 AMMSA. The authors particularly want to thank Dr. S.L. Lehoczky for his help and support.

References

[1] P.M. Amirtharaj. "Mercury Cadmium Telluride," in *Handbook of Optical Constants of Solids II*, pp. 655-686. Academic Press, 1991.

[2] W.M. Bullis, D.G. Seiler, A.C. Diebold. *Semiconductor Characterization--Present Status and Future Needs*. American Institute of Physics, Woodbury, NY (1996).

[3] L.Q. Qian, and B.W. Wessels. *Appl. Phys. Lett. 58*, 1295-1296 (1991).

[4] L.Q. Qian, and B.W. Wessels. *Appl. Phys. Lett. 58*, 2538-2539 (1991).

[5] J. D. Patterson, Analysis of scanning tunneling optical spectroscopy and infrared transmission-edge measurement for localized compositional determination of crystals of Mercury Cadmium Telluride, Mercury Zinc Telluride, and Mercury Zinc Selenide, *Final Report to UNIVERSITIES SPACE RESEARCH ASSOCIATION*. Period Covered by the Report: February 3, 1997 to May 31, 1998. Subcontract Number: 3537-000-05.

[6] B. Li, J.H. Chu, Y. Chang, Y.S. Gui, and D.Y Tang. *Infrared Physics & Technology 37*, 523-531 (1996).

[7] E.O. Kane. *J. Phys. Chem. Solids 1*, 249-261 (1957).

[8] W.W. Anderson. *Infrared Physics 20*, 363-372 (1980).

[9] Vaidya Nathan. *Journal of Applied Physics 83*, 2812-2814 (1998).

[10] S.L. Lehoczky, F.R. Szofran, and B.G. Martin. NASA CR-161598, “Advanced Methods for Preparation and Characterization of Infrared Detector Materials, Part I.” July 5, 1981.

[11] J.D. Patterson and J.G. Mantovani. *SPIE 3123* (*Materials Research in Low Gravity,* Ed. by N. Ramachandran), 75-83 (1997).

[12] R.M. Feenstra, and J.A. Stroscio. *J. Vac. Sci. Tech. B5*, pp. 923-929 (1987).

[13] J.L. Pautrat and N. Maguea. *Properties of Narrow Gap Cadmium-Based Compounds*, Ed. by Peter Capper, pp. 75-79, *IEE*, INSPEC, 1994.

[14] G. L. Hansen, J. L. Schmit, and T. N. Casselman. *J. Appl. Phys. 53*, 7099-7101 (1982).

[15] J. P. Laurenti, J. Camassel, A. Bouhemadou, B. Toulouse, R. Legros, and A. Lusson. *J. Appl. Phys. 67(10)*, 6454-6460 (1990).

[16] D. G. Seiler, J. R. Lowney, C. L. Littler, M. R. Loloee. *J. Vac. Science and Technology A8*, 1237-1244 (1990).

[17] J. Chu, B. Li, K. Liu, and D. Tang. *J. Appl. Phys. 75(2)*,1234-1235 (1994).

[18] E. Finkman and S. E. Schacham. *J. of Appl. Physics. 56*, 2896-2900 (1984).

[19] B. Toulouse, R. Granger, S. Rolland, and R. Triboulet. *J. Physique 48*, 247-251 (1987).

[20] A. B. Chen and A. Sher. *Semiconductor Alloys*, Plenum, 1995 (Interpolated).